Energy & Environmental Science

Cite this: *Energy Environ. Sci.*, 2012, **5**, 9747

www.rsc.org/ees

COMMUNICATION

Terephthalonitrile-derived nitrogen-rich networks for high performance supercapacitors†

Long Hao,[a] Bin Luo,[a] Xianglong Li,[a] Meihua Jin,[a] Yan Fang,[a] Zhihong Tang,[b] Yuying Jia,[a] Minghui Liang,[a] Arne Thomas,[c] Junhe Yang[b] and Linjie Zhi*[ab]

Received 11th July 2012, Accepted 21st September 2012
DOI: 10.1039/c2ee22814a

A novel high performance electrode material for supercapacitor applications, terephthalonitrile-derived nitrogen-rich network (TNN), is developed successfully *via* temperature-dependent cross-linking of terephthalonitrile monomers. This work opens up a new window for seeing a versatile modular toolbox derived from various aromatic nitrile monomers for developing better electrode materials in the future.

Supercapacitors, as a unique class of electrical energy storage devices, have been widely studied around the world in recent years in view of their simple principle of operation, high charge–discharge rate, excellent reversibility, and long cycle life.[1–5] However, their energy density is still very low in comparison to batteries.[6] It is well known that the energy density (E) of supercapacitors strongly depends on their specific capacitance (C) and nominal voltage according to the equation $E = CV^2/2$. To improve the energy density of supercapacitors, one of the most efficient strategies is therefore to improve their specific capacitance, for example, by increasing the surface area of electrode materials,[7–10] tuning their pore size distribution,[11,12] adding metal oxides with pseudo-capacitive effects,[13–16] as well as introducing heteroatoms including nitrogen,[17,18] oxygen,[19] phosphorus,[20] and boron[21] into the electrode. Among these existing approaches, the introduction of nitrogen into the electrode materials is attracting considerable attention since it not only enables the enhancement of conductivity, wettability, and electro-active surface area of the electrode, but also endows the electrode with pseudo-capacitance and thus further improves their electrochemical performance.[18,22,23]

On the other hand, porous organic polymers (POPs), a type of highly cross-linked polymers containing light elements (*e.g.* C, H, O, N, and B) and nanopores,[24–26] have emerged as versatile substances, applicable in many fields such as gas storage,[27] heterogeneous catalysis,[28] photocatalysis,[29] and photoconductivity.[30] For example, a kind of nitrogen-rich POPs, called covalent triazine-based frameworks-1 (CTFs-1), has been synthesized through trimerization reactions of terephthalonitrile monomers,[31–33] and successfully engaged in gas storage,[31] dye sorption,[34] and as catalyst support.[35,36] The promising functionalities of these POPs are suggested to be attributed to their intrinsic features including high surface area, well-defined pore structure, and heteroatom-doped organic skeleton, all of which originate from the precursor-defined bottom-up synthetic approaches widely used for their synthesis. Although POPs hold the above-mentioned features that are definitely favorable for the development

[a]*National Center for Nanoscience and Technology, Zhongguancun, Beiyitiao No. 11, 100190, Beijing, P. R. China. E-mail: zhilj@nanoctr.cn; Fax: +86 10 82545578; Tel: +86 10 82545578*
[b]*School of Materials Science and Engineering, University of Shanghai for Science and Technology, Jungong Road 516, 200093, Shanghai, P. R. China*
[c]*Department of Chemistry, Technische Universität Berlin, Englische Str. 20, D-10587 Berlin, Germany*

† Electronic supplementary information (ESI) available: Experimental details, Fig. S1–S11, and Tables S1 and S2. See DOI: 10.1039/c2ee22814a

Broader context

With the deepening global energy crisis, diverse renewable energy sources are emerging, which simultaneously drive the search for new energy storage systems. In this context, supercapacitors, a class of electrical energy storage devices, have been touted as a commodity bridging the performance disparity between batteries with high energy density and capacitors with high power density, in view of their simple principle of operation, high power density, excellent reversibility, and long cycle life. Porous organic polymers (POPs), a type of highly cross-linked polymers, hold many favorable advantages for the development of electrode materials in supercapacitors, including high surface area, well-defined pore structure, and heteroatom-doped monomer-designated organic skeleton, but have yet to be targeted mostly due to their poor conductivity. In this communication, amorphous terephthalonitrile-derived nitrogen-rich networks (TNNs), a kind of POPs, are successfully engineered into electrode materials in supercapacitors for the first time, and the excellent energy storage performances of these TNNs have been achieved, which are assumed to be closely associated with their controlled molecular-level structural transformations during the bottom-up synthetic processes.

of high-performance electrode materials in supercapacitors, the pioneering example of investigating the function of POPs as electrode materials for supercapacitors remains scarce,[37,38] mostly because of their relatively low conductivity. Recent studies show that amorphous networks with adjustable pore size distribution and ultrahigh surface area can be obtained by dynamic reorganization of the terephthalonitrile-derived materials *via* facilely varying the reaction conditions.[39] Whereas the conductivity of these amorphous CTFs-1 analogues was not targeted at that moment, the result evidently suggested the feasibility to further tailor the structure and property of these terephthalonitrile-derived networks, for example, specifically to tune their electrical conductivity without sacrificing their intrinsic advantages towards the development of novel terephthalonitrile-derived networks as electrode materials in supercapacitors.

Based on these considerations, we revisit CTFs-1 analogues, amorphous terephthalonitrile-derived nitrogen-rich networks (denoted as TNNs), to explore their potential as electrode materials in high performance supercapacitors. To the best of our knowledge, this is the first time that these CTFs-1 analogues are engineered into electrode materials in supercapacitors. More importantly, by tuning the synthesis temperature, the TNN-based electrodes can afford surprisingly high specific capacitances (*e.g.*, in the three-electrode system: 298 F g^{-1} at 0.2 A g^{-1} and 220 F g^{-1} at 10 A g^{-1}; in the two-electrode system: 220 F g^{-1} at 0.2 A g^{-1} and 173 F g^{-1} at 10 A g^{-1}) and excellent cycling stabilities. The striking electrochemical performances of TNNs are suggested to benefit from the molecular-level structural transformation occurred, which induces the combined characteristics of TNNs including tunable chemical and pore structures as well as adaptable electrical conductivities.

TNNs were synthesized at 400, 450, 500, 550, 600, 650, and 700 °C under ionothermal conditions[39,40] ($ZnCl_2$ as solvent and catalyst) with terephthalonitrile as the monomer (Scheme 1, also see details in the ESI†), and the materials prepared are designated as TNNs-400, TNNs-450, TNNs-500, TNNs-550, TNNs-600, TNNs-650, and TNNs-700, respectively. As a control, the CTFs-1 were synthesized following the reported method as well.[31] As shown in Fig. S1,† the powder X-ray diffraction (XRD) patterns of TNNs show no distinguishable peaks, indicative of their amorphous nature. The modalities of TNNs were further characterized by means of field-emission scanning electron microscopy (FE-SEM) and field-emission transmission electron microscopy (FE-TEM). As shown in Fig. S2,† the TNNs-400 show a quite regular and laminar modality, which is similar to the two-dimensional layered structure of CTFs-1. As the synthesis temperature increases, both TNNs-550 and TNNs-700 clearly exhibit much disordered modalities, which resemble those of three-dimensional porous materials. Although the increase of synthesis temperature has resulted in various modalities of TNNs, it should be worth noting that the chemical and pore structures of TNNs are extremely uniform. As a representative example, those of TNNs-550 are exhibited in Fig. 1. It is found that the TNNs-500 are composed of uniform porous networks as revealed by the high-resolution TEM image (Fig. 1a). The scanning transmission electron microscopy (STEM) and elemental mapping images on carbon and nitrogen further demonstrate the homogeneous distribution of nitrogen in the skeletons of TNNs-550 (Fig. 1b). In addition, elemental analyses indicate that the nitrogen content of TNNs decreases from 12.44% to 5.75% when the synthesis temperature changes from 400 °C to 700 °C (Fig. S3†), which suggests that the synthesis temperature greatly affects the composition and thus the chemical structure of TNNs.

The pore structures of all these TNNs were also characterized by the nitrogen adsorption/desorption measurement at 77 K. The isotherm of TNNs-400 is type I, showing that the TNNs-400 only contain micropores. As the synthesis temperature increases, the isotherm gradually changes from type I to type IV, indicative of the formation and propagation of mesopores (Fig. 2a). Interestingly, the Brunauer–Emmett–Teller (BET) surface area tends to increase with the pore transformation towards mesopores, which is summarized in Table S1.† The pore size distributions of TNNs were further determined based upon the density functional theory (DFT), which clearly demonstrates that a significant amount of additional mesopores have formed beside the micropores, when the synthesis temperature increases (Fig. 2b and Table S1†).

To evaluate the electrochemical performances of TNNs, a conventional three-electrode system was used, which consisted of a

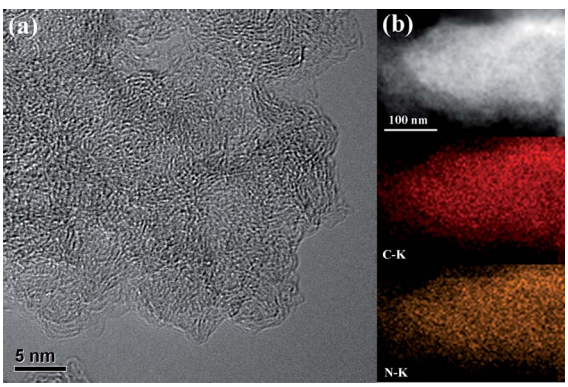

Fig. 1 (a) High-resolution TEM image of TNNs-550. (b) STEM and elemental mapping images of TNNs-550.

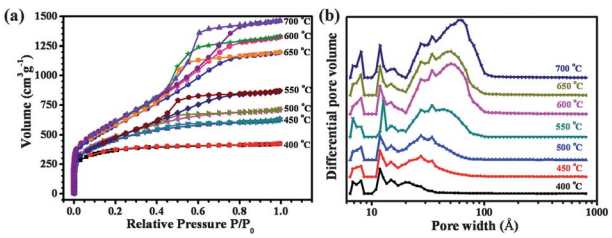

Fig. 2 (a) Nitrogen adsorption–desorption isotherms of TNNs. (b) Pore size distributions of TNNs.

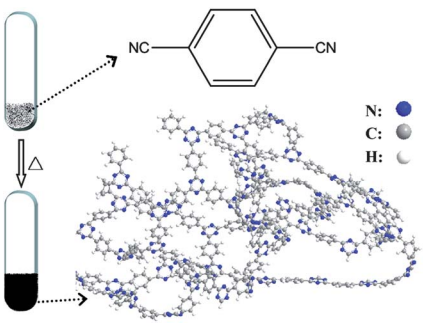

Scheme 1 Illustration of the synthesis procedure of TNNs.

TNN-based working electrode (85 wt% TNNs, 10 wt% carbon black and 5 wt% polytetrafluoroethylene (PTFE)), an aqueous Ag/AgCl electrode as the reference electrode, a platinum sheet as the counter electrode, and 1 M H_2SO_4 as the electrolyte (see ESI†). Cyclic voltammetry (CV) curves for all these TNNs at scan rates of 10 mV s^{-1} and 100 mV s^{-1} are shown in Fig. 3a and S4,† respectively. It is observed that the CV curves display quasi-rectangular shape when the synthesis temperature is higher than 500 °C, suggesting the quite decent capacitive characteristics of TNNs synthesized at a higher temperature (*e.g.*, above 500 °C). Furthermore, broad redox peaks are superposed in these CV curves, which may be associated with the nitrogen-containing functionalities existing in the skeletons of TNNs as the elemental analyses implied. It should be noted that the careful comparison between these CV curves reveals that the TNNs-550-based electrode possesses the highest current density under the same measurement conditions. Galvanostatic charge–discharge experiments were carried out to further validate the above observation. Fig. 3b shows the typical charge–discharge curves of TNNs at a current density of 10 A g^{-1}, and other results at different current densities are also exhibited in Fig. S5.† On the one hand, it is much clear that the charge and discharge curves at current densities from 0.2 A g^{-1} to 10 A g^{-1} show nearly triangular shapes when the synthesis temperature is 550 °C or higher, which suggests that the fast ion transport and quick electron propagation occurred within these TNN electrodes. On the other hand, the TNNs-550 electrode displays the highest specific capacitance, which is well consistent with the above CV results. The considerable variations in specific capacitance values (Fig. 3c), which are extracted from the discharge slopes and calculated based on the active material TNNs (see the ESI†), distinctly suggest that the electrochemical performance is closely related to the synthesis temperature of TNNs. Specifically, when the synthesis temperature increases, the specific capacitance at a current density of 0.2 A g^{-1} first increases from 248 F g^{-1} (TNNs-400), 276 F g^{-1} (TNNs-450), and 285 F g^{-1} (TNNs-500) to 298 F g^{-1} (TNNs-550), and then decreases to 263 F g^{-1} (TNNs-600), 273 F g^{-1} (TNNs-650), and 243 F g^{-1} (TNNs-700). Notably, the achieved capacitance values are much higher than those reported under similar testing conditions for other elaborately designed carbonaceous materials such as activated carbon, carbon nanotubes, and carbon foams,[41–44] which mark their great potential as electrode materials in supercapacitors. Furthermore, Fig. 3c also shows that the specific capacitance values of both TNNs-400 and TNNs-450 decrease much quicker than other TNNs as the current density increases, which may be associated with their lower synthesis temperature. Electrochemical impedance spectroscopy (EIS) was used to elucidate the above observations. The Nyquist plots (Fig. 3d) reveal that the resistance of the TNN electrode highly depends on the synthesis temperature. The equivalent series resistances are further extracted[45] and summarized in Fig. S6.† While the synthesis temperatures of both 400 °C and 450 °C make the series resistances of the TNN electrodes quite high (3.66 Ω and 2.68 Ω, respectively), the synthesis temperature of 550 °C or higher endows the TNN electrode with very small series resistances (1.88, 1.49, 1.53, and 1.53 Ω, respectively, for 550, 600, 650, and 700 °C) favorable for supercapacitor applications. The significantly higher resistances of TNNs-400 and TNNs-450 electrodes, which are induced by their synthesis temperature, may be responsible for their dramatically low specific capacitance values when the current density increases (Fig. 3c), and also for the temperature-related ohmic drop (or IR drop) observed in the discharge curves (Fig. 3b and S5†). In addition, the TNN electrodes are observed to be very stable. As an example, the TNNs-550 electrode was charged/discharged at a current density of 10 A g^{-1} for 5000 cycles, showing no detectable degradation and maintaining a specific capacitance of about 220 F g^{-1} (Fig. S7†). It can be concluded that the TNNs are capable of exhibiting both high specific capacitance and excellent cycling stability given a suitable synthesis temperature.

In order to further demonstrate the electrochemical performances of these TNNs, we finally picked some of the TNNs based on their series resistances and assembled them into a conventional two-electrode system,[46] which consisted of two symmetric working electrodes (85 wt% TNNs, 10 wt% carbon black and 5 wt% PTFE) and 1 M H_2SO_4 as the electrolyte (see details in the ESI†). Consistent with those observed in the above three-electrode system, both quasi-rectangular CV curves (Fig. 4a and S8†) and nearly triangular symmetric galvanostatic charge–discharge curves (Fig. S9† and the inset in Fig. 4b) clearly highlight the superior supercapacitance performance of these TNNs assembled into symmetric supercapacitors. As shown in Fig. 4b, the tendency of the capacity change along with the reaction temperature is the same as the results from the three-electrode system. Notably, the TNNs-550 consistently show the best performance with the specific capacitance of 220 F g^{-1} at 0.2 A g^{-1} and 173 F g^{-1} at 10 A g^{-1}.

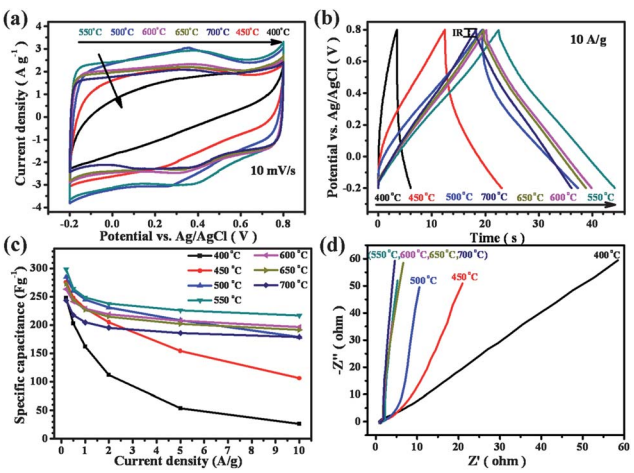

Fig. 3 Electrochemical properties of TNN-based electrodes measured in a three-electrode system. (a) Cyclic voltammograms, (b) galvanostatic charge–discharge curves, (c) specific capacitances at various current densities, and (d) Nyquist plots (AC frequency ranges from 100 000 to 0.01 Hz) of TNN-based electrodes.

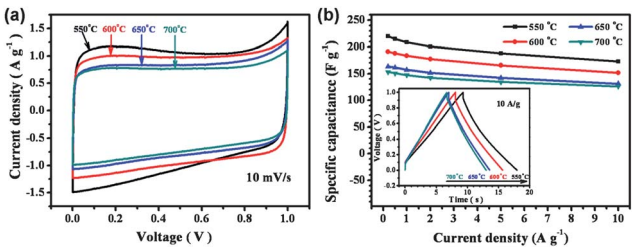

Fig. 4 Electrochemical properties of TNN-based electrodes measured in a two-electrode system. (a) CV and (b) specific capacitances at various current densities with galvanostatic charge–discharge curves in the inset.

X-ray photoelectron spectroscopy (XPS) analyses of TNNs were performed in order to further explore the origin of the temperature-dependent electrochemical performances of TNN electrodes. The N1s XPS results of TNNs (Fig. S10†) reveal that four distinct N configurations exist in the skeletons of TNNs: pyridinic N (397.98–398.40 eV, N_i), pyrrolic N (399.60–399.99 eV, N_{ii}), quaternary N (400.86–401.19 eV, N_{iii}), and N-oxide (402.65–403.94 eV, N_{iv}),[47–49] while those of CTFs-1 show N_i, N_{ii}, and negligible N_{iv} (Fig. S11†). The significant difference in N configurations of TNNs and CTFs-1 suggests that some rearrangement reactions or even decomposition reactions may occur under the synthesis conditions for TNNs.[39,50,51] The atomic ratios of the four N-configurations (N_x, x stands for i, ii, iii and iv) in TNNs are further evaluated from the deconvolution of N1s peaks for TNNs (Fig. S10 and Table S2†),[52,53] and the results are plotted as a function of synthesis temperature in Fig. 5a. Notably, the ratios of both N_i and N_{ii} tend to decrease when the synthesis temperature increases; in contrast, the ratios of N_{iii} and N_{iv} increase with increasing synthesis temperature. The results indicate that a low synthesis temperature is helpful for the formation of N_i and N_{ii} and yet the formation and propagation of N_{iii} and N_{iv} require a relatively high temperature. That is, the synthesis temperature strongly dominates the N configurations in TNNs. Combined with synthesis temperature-related N contents of TNNs as shown by elemental analyses, it is assumed that the π-conjugated system in the structures of TNNs is randomly extended at relatively higher temperatures, thus making the molecular-level structural transformation from an ordered structure to an extended one (like CTFs-1 to TNNs in Fig. 5b). This transformation may be responsible for the temperature-dependent changes of modality, pore structure, and resistance of TNNs, all of which finally enable the modulations in the electrochemical performances of TNN electrodes. More specifically, as the synthesis temperature increases: (1) under 550 °C, the molecular-level structural transformation, including the increase in N_{iii} and N_{iv} configurations relative to N_i and N_{ii}, leads to the decrease in TNN resistances, which facilitates the electron propagation, and being a key to enhancing the electrochemical performances of TNN electrodes. In addition, this structural transformation endows TNNs with irregular modalities, large ion-accessible surface areas, and optimized combination of micropores and mesopores, which may also contribute to the significant improvement of the electrochemical performances of TNN electrodes; and (2) above 550 °C, the decrease in nitrogen content degrades the fast surface redox reactions and wettability of TNNs.[18,22] Also, the molecular-level structural transformation occurred in this temperature range may also induce pore size distributions unfavorable for the adsorption/desorption of solvated ions.[10–12,54] Both factors may be responsible for the gradually worsened electrochemical performances with the increase in synthesis temperature, whereas the modality, specific surface area, and resistance still play positive roles in the TNN-based electrodes.

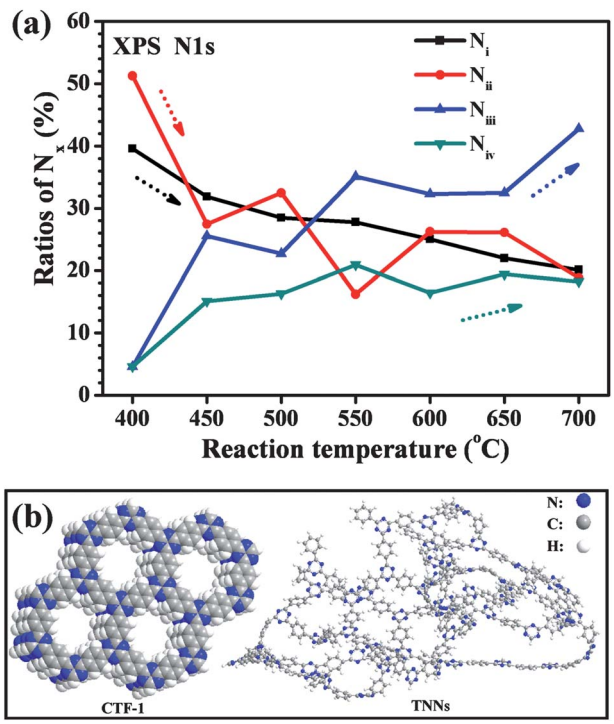

Fig. 5 (a) The ratios of four N-configurations (N_x) in TNNs. (b) Illustration of the ordered structure of CTFs-1 and the possible structure of TNNs synthesized at relatively high temperatures.

In summary, terephthalonitrile-derived nitrogen-rich networks (TNNs) have been successfully developed as high-performance electrode materials for supercapacitors. An efficient combination of nitrogen-rich functions, large ion-accessible surface area, micropore and mesopore interconnection, and low resistance, which are crucial for TNNs to be excellent electrode materials, is achieved simply by altering the synthesis temperatures. The TNNs obtained at 550 °C exhibit both high specific capacitance and excellent cycling durability, demonstrating attractive properties for practical applications. This work also opens up a new window for seeing a versatile modular toolbox derived from various aromatic nitrile monomers in the development of high performance electrode materials for supercapacitors and other energy storage devices as well.

Acknowledgements

Financial support from the National Natural Science Foundation of China (Grant no. 20973044, 21173057, 51102168, and 21103030), the Ministry of Science and Technology of China (no. 2009DPA41220 and no. 2012CB933403), the Chinese Academy of Sciences (no. KJCX2-YW-H21), and Shanghai Natural Science Foundation (no. 11ZR1424700) is acknowledged.

Notes and references

1 M. Winter and R. J. Brodd, *Chem. Rev.*, 2004, **104**, 4245–4270.
2 J. R. Miller and P. Simon, *Science*, 2008, **321**, 651–652.
3 L. L. Zhang and X. S. Zhao, *Chem. Soc. Rev.*, 2009, **38**, 2520–2531.
4 C. Liu, F. Li, L.-P. Ma and H.-M. Cheng, *Adv. Mater.*, 2010, **22**, E28–E62.
5 K. Sheng, Y. Sun, C. Li, W. Yuan and G. Shi, *Sci. Rep.*, 2012, **2**, 247.
6 P. Simon and Y. Gogotsi, *Nat. Mater.*, 2008, **7**, 845–854.
7 G. Ning, Z. Fan, G. Wang, J. Gao, W. Qian and F. Wei, *Chem. Commun.*, 2011, **47**, 5976–5978.
8 S. L. Candelaria, R. Chen, Y.-H. Jeong and G. Cao, *Energy Environ. Sci.*, 2012, **5**, 5619–5637.
9 H.-L. Jiang, B. Liu, Y.-Q. Lan, K. Kuratani, T. Akita, H. Shioyama, F. Zong and Q. Xu, *J. Am. Chem. Soc.*, 2011, **133**, 11854–11857.
10 B. Liu, H. Shioyama, H. Jiang, X. Zhang and Q. Xu, *Carbon*, 2010, **48**, 456–463.
11 C. Largeot, C. Portet, J. Chmiola, P.-L. Taberna, Y. Gogotsi and P. Simon, *J. Am. Chem. Soc.*, 2008, **130**, 2730–2731.
12 J. Chmiola, G. Yushin, Y. Gogotsi, C. Portet, P. Simon and P. L. Taberna, *Science*, 2006, **313**, 1760–1763.

13 L. Bao, J. Zang and X. Li, *Nano Lett.*, 2011, **11**, 1215–1220.
14 C.-C. Hu, K.-H. Chang, M.-C. Lin and Y.-T. Wu, *Nano Lett.*, 2006, **6**, 2690–2695.
15 Y. Liang, M. G. Schwab, L. Zhi, E. Mugnaioli, U. Kolb, X. Feng and K. Mullen, *J. Am. Chem. Soc.*, 2010, **132**, 15030–15037.
16 W. Lv, F. Sun, D.-M. Tang, H.-T. Fang, C. Liu, Q.-H. Yang and H.-M. Cheng, *J. Mater. Chem.*, 2011, **21**, 9014–9019.
17 D. Hulicova-Jurcakova, M. Kodama, S. Shiraishi, H. Hatori, Z. H. Zhu and G. Q. Lu, *Adv. Funct. Mater.*, 2009, **19**, 1800–1809.
18 G. Lota, K. Lota and E. Frackowiak, *Electrochem. Commun.*, 2007, **9**, 1828–1832.
19 D. Hulicova-Jurcakova, M. Seredych, G. Q. Lu and T. J. Bandosz, *Adv. Funct. Mater.*, 2009, **19**, 438–447.
20 D. Hulicova-Jurcakova, A. M. Puziy, O. I. Poddubnaya, F. Suarez-Garcia, J. M. D. Tascon and G. Q. Lu, *J. Am. Chem. Soc.*, 2009, **131**, 5026–5027.
21 X. Zhao, A. Wang, J. Yan, G. Sun, L. Sun and T. Zhang, *Chem. Mater.*, 2010, **22**, 5463–5473.
22 P. J. Hall, M. Mirzaeian, S. I. Fletcher, F. B. Sillars, A. J. R. Rennie, G. O. Shitta-Bey, G. Wilson, A. Cruden and R. Carter, *Energy Environ. Sci.*, 2010, **3**, 1238–1251.
23 G. Lota, K. Fic and E. Frackowiak, *Energy Environ. Sci.*, 2011, **4**, 1592–1605.
24 N. B. McKeown and P. M. Budd, *Macromolecules*, 2010, **43**, 5163–5176.
25 Y. Zhang and S. N. Riduan, *Chem. Soc. Rev.*, 2012, **41**, 2083–2094.
26 A. Thomas, *Angew. Chem., Int. Ed.*, 2010, **49**, 8328–8344.
27 R. Dawson, E. Stoeckel, J. R. Holst, D. J. Adams and A. I. Cooper, *Energy Environ. Sci.*, 2011, **4**, 4239–4245.
28 J.-X. Jiang, C. Wang, A. Laybourn, T. Hasell, R. Clowes, Y. Z. Khimyak, J. Xiao, S. J. Higgins, D. J. Adams and A. I. Cooper, *Angew. Chem., Int. Ed.*, 2011, **50**, 1072–1075.
29 X. C. Wang, K. Maeda, A. Thomas, K. Takanabe, G. Xin, J. M. Carlsson, K. Domen and M. Antonietti, *Nat. Mater.*, 2009, **8**, 76–80.
30 X. Ding, J. Guo, X. Feng, Y. Honsho, J. Guo, S. Seki, P. Maitarad, A. Saeki, S. Nagase and D. Jiang, *Angew. Chem., Int. Ed.*, 2011, **50**, 1289–1293.
31 P. Kuhn, M. Antonietti and A. Thomas, *Angew. Chem., Int. Ed.*, 2008, **47**, 3450–3453.
32 P. Kuhn, A. Thomas and M. Antonietti, *Macromolecules*, 2008, **42**, 319–326.
33 W. Zhang, C. Li, Y.-P. Yuan, L.-G. Qiu, A.-J. Xie, Y.-H. Shen and J.-F. Zhu, *J. Mater. Chem.*, 2010, **20**, 6413–6415.
34 P. Kuhn, K. Kruger, A. Thomas and M. Antonietti, *Chem. Commun.*, 2008, 5815–5817.
35 C. E. Chan-Thaw, A. Villa, P. Katekomol, D. Su, A. Thomas and L. Prati, *Nano Lett.*, 2010, **10**, 537–541.
36 C. E. Chan-Thaw, A. Villa, L. Prati and A. Thomas, *Chem.–Eur. J.*, 2011, **17**, 1052–1057.
37 X. L. Feng, Y. Y. Liang, L. J. Zhi, A. Thomas, D. Q. Wu, I. Lieberwirth, U. Kolb and K. Mullen, *Adv. Funct. Mater.*, 2009, **19**, 2125–2129.
38 Y. Kou, Y. Xu, Z. Guo and D. Jiang, *Angew. Chem., Int. Ed.*, 2011, **50**, 8753–8757.
39 P. Kuhn, A. l. Forget, D. Su, A. Thomas and M. Antonietti, *J. Am. Chem. Soc.*, 2008, **130**, 13333–13337.
40 G. L. Cui, Y. S. Hu, L. J. Zhi, D. Q. Wu, I. Lieberwirth, J. Maier and K. Mullen, *Small*, 2007, **3**, 2066–2069.
41 Z. Li, L. Zhang, B. S. Amirkhiz, X. Tan, Z. Xu, H. Wang, B. C. Olsen, C. M. B. Holt and D. Mitlin, *Adv. Energy Mater.*, 2012, **2**, 431–437.
42 L. Zhao, L.-Z. Fan, M.-Q. Zhou, H. Guan, S. Qiao, M. Antonietti and M.-M. Titirici, *Adv. Mater.*, 2010, **22**, 5202–5206.
43 X. Zhao, B. T. T. Chu, B. Ballesteros, W. Wang, C. Johnston, J. M. Sykes and P. S. Grant, *Nanotechnology*, 2009, **20**, 065605.
44 J. Lee, *Phys. Chem. Chem. Phys.*, 2012, **14**, 5695–5704.
45 E. J. Ra, E. Raymundo-Piñero, Y. H. Lee and F. Béguin, *Carbon*, 2009, **47**, 2984–2992.
46 K. Xie, X. Qin, X. Wang, Y. Wang, H. Tao, Q. Wu, L. Yang and Z. Hu, *Adv. Mater.*, 2012, **24**, 347–352.
47 H. Konno, H. Onishi, N. Yoshizawa and K. Azumi, *J. Power Sources*, 2010, **195**, 667–673.
48 D. Usachov, O. Vilkov, A. Grueneis, D. Haberer, A. Fedorov, V. K. Adamchuk, A. B. Preobrajenski, P. Dudin, A. Barinov, M. Oehzelt, C. Laubschat and D. V. Vyalikh, *Nano Lett.*, 2011, **11**, 5401–5407.
49 C. E. Chan-Thaw, A. Villa, G. M. Veith, K. Kailasam, L. A. Adamczyk, R. R. Unocic, L. Prati and A. Thomas, *Chem.–Asian J.*, 2012, **7**, 387–393.
50 T. V. Balashova, G. V. Khoroshenkov, D. M. Kusyaev, I. L. Eremenko, G. G. Aleksandrov, G. K. Fukin and M. N. Bochkarev, *Russ. Chem. Bull.*, 2004, **53**, 825–829.
51 R. E. Del Sesto, A. M. Arif, J. J. Novoa, I. Anusiewicz, P. Skurski, J. Simons, B. C. Dunn, E. M. Eyring and J. S. Miller, *J. Org. Chem.*, 2003, **68**, 3367–3379.
52 H. M. Jeong, J. W. Lee, W. H. Shin, Y. J. Choi, H. J. Shin, J. K. Kang and J. W. Choi, *Nano Lett.*, 2011, **11**, 2472–2477.
53 D. Hulicova, J. Yamashita, Y. Soneda, H. Hatori and M. Kodama, *Chem. Mater.*, 2005, **17**, 1241–1247.
54 J. Chmiola, C. Largeot, P.-L. Taberna, P. Simon and Y. Gogotsi, *Angew. Chem., Int. Ed.*, 2008, **120**, 3440–3443.